

Photoluminescence Plasmonic Enhancement of Single Quantum Dots Coupled to Gold Microplates

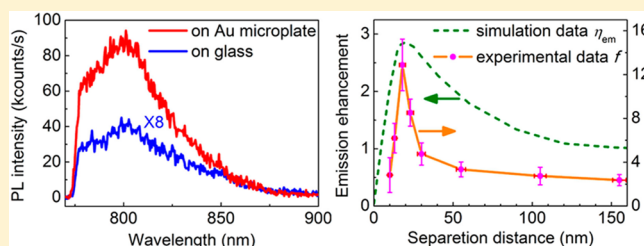
Min Song, Botao Wu,* Gengxu Chen, Yan Liu, Xueting Ci, E Wu, and Heping Zeng*

State Key Laboratory of Precision Spectroscopy, East China Normal University, Shanghai, 200062, China

Supporting Information

ABSTRACT: Optical properties of quantum dots can be drastically changed by surface plasmons excited in neighboring metallic nanostructures. Here we investigated the photoluminescence enhancement dependence of single quantum dots on the separation distance with Au microplates by a single particle spectroscopy. The quantum dot–Au microplate hybrid structures provided a photoluminescence enhancement of up to ~ 16 -fold when the separation distance between the surface of Au microplate and the center of QD was 18 ± 1.9 nm.

Accordingly, the lifetime of those quantum dots was shortened compared with the ones on glass plates directly. Theoretical simulation revealed that the variation of photoluminescence enhancement was closely dependent on the separation distance between the QD and the Au microplate, in good agreement with the experimental results.



INTRODUCTION

Surface plasmons (SPs) are electromagnetic waves coupled to the collective oscillations of free electrons on metal surface. The resonant excitation of SPs on metallic nanostructures provides ways to localize, guide, and manipulate electromagnetic waves beyond the diffraction limit and to tailor light-matter interactions down to nanometer scale, which has enabled a rich variety of new fundamental techniques and applications including plasmonic photovoltaic cells,¹ surface-plasmon enhanced spectroscopies,^{2–9} photochemistry,^{10–12} bioimaging and therapeutics,^{13,14} sensing,^{15,16} superlenses,¹⁷ nanolasers,¹⁸ and quantum optics.^{19–21} Taking the advantage of SPs excited in neighboring metallic nanostructures, optical properties of semiconductor quantum dots (QDs) in particular, can be significantly modified.^{22–43} Besides the desirable intrinsic properties and the specially designed micro/nano structures, the relative position of QDs with the metallic structures, particularly the distance, plays a crucial role in the achievement of strong photoluminescence (PL) enhancement of the QDs. For instance, the effective coupling between a single QD and a metal film could be achieved by optimizing the thickness of the polymer layer between the isolated QD and the metallic film surface.^{23–26} Comparing with the QDs coupled with metallic nanoparticles by constructing complex chemical linkage or dielectric shells in between,^{28–32} the coupling between QDs and metal films can be easily achieved by a simple spin-coating method.^{22–27} However, metal films are usually fabricated using metal evaporation and deposition method with polycrystalline structure and rough surface. It has been reported that the strips fabricated by metal deposition suffered larger energy loss for surface plasmon compared with metal nanowires synthesized by a wet chemical method with single crystal structures and smooth surfaces due to scattering off the rough surfaces and the

grain boundaries in the strips.⁴⁴ Moreover, surface propagating plasmon modes on metallic films could not effectively couple to light due to the momentum mismatch between photons and electron motions.²⁷ As an alternative, Au microplates, which are synthesized by a wet chemical method and grow as single crystals with the size of tens of micrometers,^{45,46} shows advantages over metal films, such as the regular single-crystalline structure which could reduce the energy loss of SPs and the microplate boundary for localizing SPs propagating. Comparing with the QDs in size of several nanometers, Au microplates are equivalent to a very large plane which can be used as a simple and effective substrate for surface enhanced fluorescence.

In this paper, we reported the engineering of coupling between single CdSeTe/ZnS QDs and single Au microplates, and investigated the dependence of PL properties of the QDs on the separation distance between the surface of the Au microplates and the center of the QDs. By precisely controlling the thickness of poly(methyl methacrylate) (PMMA) separating layer in between, we observed gradual changes on the QD PL intensity and lifetime. Up to ~ 16 -fold PL enhancement was experimentally achieved when the separation distance was 18 ± 1.9 nm, and accordingly, the shortest PL lifetime was observed. The PL dynamics related to the separation distance was well explained by theoretical simulations based on the enhanced dipole emitter model. This hybrid structure may have potential applications in quantum light source and biological imaging.

Received: August 20, 2013

Revised: April 4, 2014

Published: April 4, 2014

EXPERIMENTAL METHODS

Au microplates were synthesized by seed growth method following the previous works.^{45,46} The reaction products were diluted with acetone and centrifuged at 2500 rpm for 20 min and then washed twice with deionized water. The products were then filtered by a microporous membrane with porous diameter of 1 μm to keep only the big-size Au microplates. Finally, the Au microplates on membrane were collected and redispersed in deionized water for further use. The morphological features of the Au microplates were characterized by an atomic force microscope (AFM, JPK NanoWizard II). The fabricated Au microplates were a mixture of hexagonal-truncated triangular shapes as shown in Figure 1a, with a

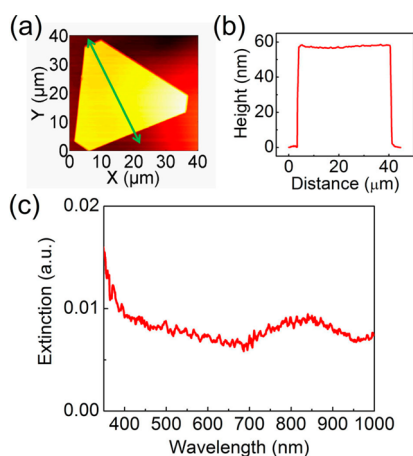


Figure 1. (a) AFM image of an Au microplate. (b) Line analysis across the Au microplate in part a. (c) Extinction spectrum of Au microplates covered by a layer of PMMA in a glass substrate.

size-distribution of $\sim 35 \pm 10 \mu\text{m}$. The Au microplates could be well dispersed with very low density and spin-coated on glass substrates without overlapping. In Figure 1b, the line analysis of AFM image indicates that the Au microplates were around 55 nm in average thickness. The surface quality of the Au microplates was examined in nanometer and micrometer scales using the AFM (Figure S1, Supporting Information), indicating a planar and smooth surface with about ± 0.5 nm fluctuation because of the seed-growth single crystal structure of the Au microplates.^{45,46} Here, the coupling of the QD–Au microplate hybrid structures is performed by PMMA films. The optical property of the Au microplates covered by a layer of PMMA film on a glass substrate was first investigated with a UV–visible–NIR spectrophotometer (JASCO V-570). Figure 1c displays optical extinction spectrum of PMMA-covered Au microplates on a glass substrate. Only one broad absorption band with the maximum absorption around 840 nm is observed, which originated from the in-plane quadrupole resonance of the Au microplates.⁴⁵

To demonstrate the PL dynamics of QDs coupled to Au microplates, we engineered the separation distance by a PMMA separation layer with nanometer-scale thickness in between. The hybrid structure samples as shown in Figure 2a were prepared as follows. First, dilute suspensions of Au microplates in deionized water were spin-coated on clean glass substrates. After drying the substrates in air, PMMA films were prepared by spin-coating at 3000 rpm for 60 s as separation layers between the Au microplates and the QDs. The thicknesses of the PMMA layers were tuned from 5 to 150 nm by changing

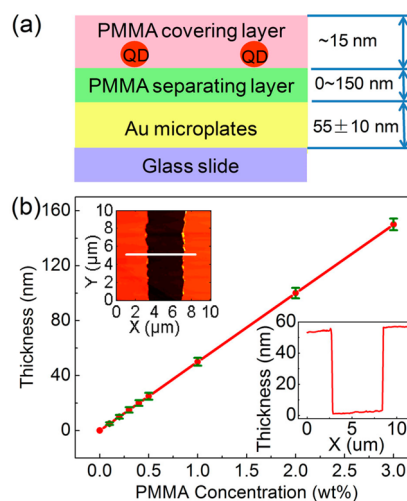


Figure 2. (a) Sample schematic and (b) Relationship between the thickness of PMMA films and the concentration of PMMA solutions. The inset in part b shows an AFM image of one groove scratched in the PMMA film with concentration of 1.0 wt % and a corresponding line analysis across this groove.

the mass concentrations of PMMA solutions by 0.1, 0.2, 0.3, 0.4, 0.5, 1.0, 2.0, and 3.0 (wt %) as shown in Figure 2b. CdSeTe/ZnS core–shell QDs with fluorescence emission centered at ~ 800 nm were used as probes to demonstrate plasmonic enhanced PL of single QD coupled to Au microplates. Transmission electron microscope (TEM) and AFM characterizations indicated that the CdSeTe/ZnS QDs had a wedgelike shape and a height of about 10 nm (Figure S2). The QDs with a concentration of 1 μM (Invitrogen, SKU# Q21771MP) were diluted to 1 nM with acetone. Then a drop of QD solution was spin-coated on the PMMA-coated Au microplates. Finally, the QDs were covered with a PMMA film of about 15 nm thickness to avoid photooxidation during laser excitation. A reference sample without Au microplates was prepared in the same way. The thicknesses of the PMMA films between Au microplates and QDs played a critical role in controlling their mutual coupling strength. Using the AFM, we checked the precision and reproducibility of the PMMA films by examining the film thickness variation for different slides with the same spin-coating procedure in a certain PMMA mass concentration, and estimated the PMMA film uniformity by examining the film thickness variation along the grooves scratched in the films across the substrate. The results indicated that when the PMMA mass concentration was below 0.5 wt %, the PMMA film thicknesses had a small fluctuation for different slides with the same spin-coating procedure, showing good precision and reproducibility. Furthermore, the film thicknesses in this concentration range also showed a good uniformity due to the small variation in the film thicknesses measured in the different locations along the grooves. However, when the PMMA mass concentration was beyond 0.5 wt %, the precision, reproducibility, and uniformity of PMMA films became worse, because the viscosity of the PMMA solutions became large with the PMMA mass concentration increasing, and as a result, it became difficult for the PMMA solutions to be uniformly spread across the substrates. To clarify whether the PMMA film thickness obtained in Figure 2b was consistent with that on Au microplates, we took the AFM images of an Au microplate without and with a PMMA layer of about 15 nm as shown in Figure S3. Detectable accumulation zone around the edge of

the Au microplate was not observed. Furthermore, the implementation of the PMMA layer did not change the Au microplate thickness. Therefore, the PMMA layer thicknesses measured with and without Au microplates were consistent. The PMMA thicknesses obtained in Figure 2b were also representative of those on top of the Au microplates. Considering the height of QDs, the separation distance between the surface of the Au microplate and the center of the QDs should be the sum of the half height of the QDs (5 nm) and the thickness of PMMA separation layer.

Using a scanning confocal microscope system, the PL properties from a single QD on single Au microplates as well as on glass plates were investigated. A 532 nm solid-state laser (continuous wave) was used as the excitation source. The laser beam was focused into diffraction-limited spot on a single QD by a high numerical aperture microscope objective (NA = 0.95, $\times 100$). The PL from the single QD was collected by the same microscope objective, and after spatial and spectral filtering sent to a silicon avalanche photodiode single-photon detector for monitoring the intensity or to a spectrometer (SpectraPro-300i, Acton Research Corporation) for spectrum analysis. The spontaneous emission decay lifetime of a single QD was measured using time correlated single photon counter (TCSPC) when the excitation laser source was replaced by a frequency-doubled mode-locked pulsed Yb-doped fiber laser. The pulse width, wavelength, power, and repetition rate were 10 ps, 520 nm, 50 μW , and 1 MHz, respectively.

RESULTS AND DISCUSSION

PL properties from single QDs on single Au microplates with PMMA separating layers of different thicknesses as well as on glass were studied by the scanning confocal microscope. The excitation laser power was maintained at about 0.28 mW in order to achieve a high signal-to-noise ratio of the QD photoluminescence while keeping the single-photon detector to work below saturation. In this way, the excitation conditions were ensured to be the same for the QDs on the glass and the Au microplates. To achieve single particle detection within the diffraction limited area of the microscope objective, the QD concentration was diluted to 1 nM so that the QDs after the spin coating dispersed very well on the PMMA films. A representative AFM image of the dispersy of the QDs on a PMMA-covered Au microplate is presented in Figure S4, from which we can see that the QDs dispersed very well and most of the interparticle distances between two QDs are beyond the radius of the diffraction limited area of the 100 \times microscope objective (about 0.12 μm). We examined the single QD PL properties on 3–4 glass slides with the same spin-coating procedure for each PMMA separation distance as well as 2–4 Au microplates for each slide. Actually Au microplates also exhibited a visible PL when excited by a 532 nm laser. Figure S5 shows fluorescence image and spectrum of an Au microplate. It could be seen that the QD fluorescence around 800 nm located the tail of the Au fluorescence spectrum, thus a short-pass filter cutting off at 780 nm was used to remove the PL from the Au microplates and other stray noise photons. To avoid the edge effect of the Au microplates, only the QDs locating close to the center of the Au microplates were examined. We chose an Au microplate around the center of the glass slide by a CCD camera. Then the fluorescence image of this Au microplate was obtained by the computer controlled scanning confocal microscope (Figure S5), in which the scanning area could be chosen at the center of the Au microplate and QD emitters

within this area were recorded. About 20 individual QDs for each sample were studied.

Parts a and b of Figure 3 show scanned fluorescence images of single QDs on a glass plate as well as on an Au microplate

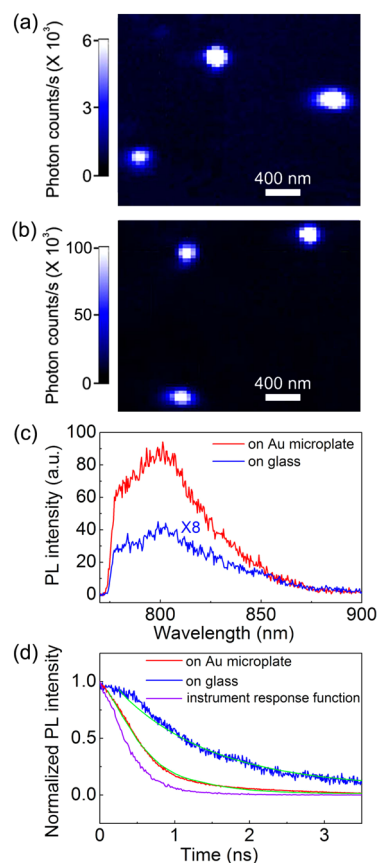


Figure 3. Confocal fluorescence images of single QDs on glass (a) and on an Au microplate with an application of about 13 nm PMMA separating layer (b). PL emission spectra (c) and decay curves with double exponential fitted curves (green curves) (d) of single QDs on glass and on an Au microplate with about 13 nm PMMA separating layer. The decay curves in part d have been deconvolved from the instrument response function.

with a 13 nm PMMA separating layer. The emission intensity of the single QDs on glass was quite low but was strongly enhanced on the Au microplate. A typical PL spectrum from a single QD on Au microplate with a 13 nm PMMA separating layer together with that of a single QD on glass is exhibited in Figure 3c, and the corresponding fluorescence decay curves are shown in Figure 3d. It could be seen that the QD PL intensity was enhanced with about 16-fold when the QD was on the Au microplate. This PL intensity enhancement value was about 3–6 times larger than that obtained in the hybrid structures of single QDs and conventional metal films.^{22,24,25} It could also be noticed that the PL spectral profiles of the QDs with and without Au microplate were identical, indicating that the spectral properties of the QD were retained. The time-resolved PL of single QDs was measured by using TCSPC technology with a pulsed laser excitation. Those PL decay curves were convolutional results of the real decay curves and the instrumental response function. A combination of the phase plane method and iterative convolution method was used in making deconvolution to obtain the real fluorescence life-

times.^{47,48} The fluorescence decay curves of the QDs on glass and on the Au microplate in Figure 3d exhibit a nonsingle exponential behavior, but can be fitted well by a double exponential decay function

$$I(t) = A_1 \exp(-t/\tau_1) + A_2 \exp(-t/\tau_2) \quad (1)$$

where τ_1 and τ_2 are the shorter and longer lifetimes of the fluorescence emitter, respectively, and A_1 and A_2 are their respective amplitudes. The double exponential decay behavior of the QD fluorescence might stem from nonradiative decay processes, e. g. Auger process, energy transfer from QDs to Au microplates (see Supporting Information for detailed discussion). The average lifetime for each sample are given by

$$\tau_m = \frac{A_1\tau_1^2 + A_2\tau_2^2}{A_1\tau_1 + A_2\tau_2} \quad (2)$$

The bare QD on glass showed an averaged lifetime $\tau_m = 1.61$ ns (blue curve in Figure 3b). In contrast, an apparent decrease of the lifetime of the single QD on the Au microplate was observed with $\tau_m = 0.57$ ns (red curve in Figure 3b). Clearly, the PL decay of the QD-Au microplate hybrid structure was faster than that of the bare QD on glass, suggesting that the PL decay rate of the QD was substantially affected by the Au microplate. Identical results in terms of PL enhancement and lifetime decrease were observed for the samples with PMMA separation layers of different thicknesses. Parts a and b of Figure 4 show the dependence of the PL intensity and the

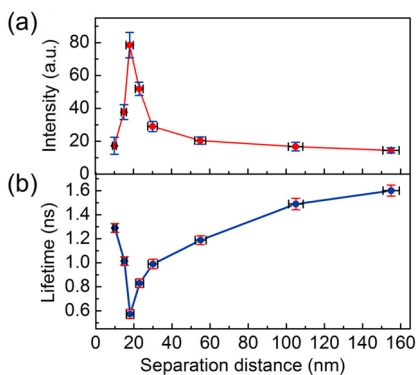


Figure 4. Dependence of PL intensity (a) and average lifetime (b) of the QDs coupled with Au microplates on the separation distance. The error bars in parts a and b were determined by the standard deviation.

average lifetime of single QDs coupled with single Au microplates on the separation distance, respectively. It could be clearly seen that with the separation distance increasing, the PL intensity first rapidly increased and then fast decreased. On the contrary, the PL average lifetime behaved the opposite way as the PL intensity. Specifically, the optimum separation distance, corresponding to the maximum PL intensity and the minimum average lifetime of single QDs (namely, a ~ 16 -fold enhancement of PL intensity and a ~ 3 -fold increase of decay rate, compared with those of the bare QDs in PMMA on glass, i.e. 6.2 kcounts/s and 1.61 ns), was 18 ± 1.9 nm. The physical insight into this behavior of the PL intensity of the QDs dependent on the separation distance will be discussed below combined with theory simulations. It was also seen that the PL intensity of the single QDs showed a little fluctuation at each separation distance. In Figure 2b, we have known that the PMMA film thickness showed a fluctuation even in the same

spin-coating procedure. As the PL intensities of the QDs strongly depended on the gap distance between the QDs and the Au microplates, especially in the near field area of surface plasmon resonance of the Au microplates, it could be expected that the QD PL intensities also had a fluctuation range. And actually when QDs were directly placed on Au microplates, the PL was completely quenched due to the ultrafast energy transference from the photoexcited QDs to the Au microplates.^{40–43}

To analyze the PL dynamics of single QDs on Au microplates, an electromagnetic model based on the interaction of a dipole and the rough surface of ellipsoid is introduced.⁴⁹ For a radiative dipole (i.e., organic dye molecules or QDs) under weak excitation (no saturation), the emission rate γ_{em} is a two-step process involving the excitation rate γ_{exc} and the emission probability represented by quantum yield $q = \gamma_r/(\gamma_r + \gamma_{nr}) = \gamma_r/\gamma_t$ with γ_r , γ_{nr} and γ_t (sum of γ_r and γ_{nr}) being the radiative, nonradiative and total decay rates, respectively.^{22,50} In this hybrid structure, Au microplates modified both steps of the QD PL process (γ_{exc} and q) by SPs coupling to light. During excitation, the incident light excited not only the QDs but also SPs in the Au microplates. The SPs enhanced local field coupled to the QDs and increased γ_{exc} . In the subsequent emission process, the presence of the Au microplates altered the quantum yield via modification of both radiative and nonradiative decay rates. According to the Purcell effect,⁵¹ QD's radiative decay rate was altered due to the changes in the local electromagnetic density of states introduced by the Au microplates. Additionally, as the separation between the QDs and the Au microplates decreased, the nonradiative rate of the QDs increased due to ultrafast energy transfers to the Au microplates.

To describe the process more quantitatively, theoretical simulations were carried out in order to investigate the variation of PL properties of the QDs on the separation distance using the finite difference time domain (FDTD) method with the software FDTD Solutions 8.4. The QD was treated as a point dipole emitter emitting at 800 nm. The refractive index of background was set to 1.46, which matched with that of PMMA that the QDs were embedded in. The γ_r , γ_{nr} , and γ_t of the point dipole emitter with different separation distances from the Au microplates were calculated, as shown in Figure 5a. The excitation enhancement η_{exc} , the quantum efficiency q , and the PL emission enhancement η_{em} of the QDs coupled to the Au microplates based on the dipole emitter model as a function of the QD-Au microplate separation were calculated according to $\eta_{exc} \approx \gamma_r/\gamma_{r,0}$, $q = \eta_{exc}/(\gamma_t/\gamma_{t,0})$, and $\eta_{em} = \eta_{exc}q$ (subscript 0 refers to the bare QD in PMMA on glass slide), respectively,^{22,50} which are displayed in Figure 5 together with the experimental PL enhancement. Figure 5b shows the calculated η_{exc} and q values as a function of the separation distance between the surface of the Au microplate and the center of the QD. It could be seen that the η_{exc} and q behaved oppositely with the separation distance. The competition between them determined the optimal separation distance, in which the highest PL intensity enhancement could be achieved. Figure 5c shows the calculated PL emission enhancement η_{em} as a function of the separation distance with the experimental data f . Here, the experimental data of PL emission enhancement was defined as I_{Au}/I_0 , where I_{Au} was the PL intensity of single QDs on Au microplates, and I_0 was that of single QDs on glass slide. In the calculation, we used the point dipole emitter to represent the QD. The separation distance used in the

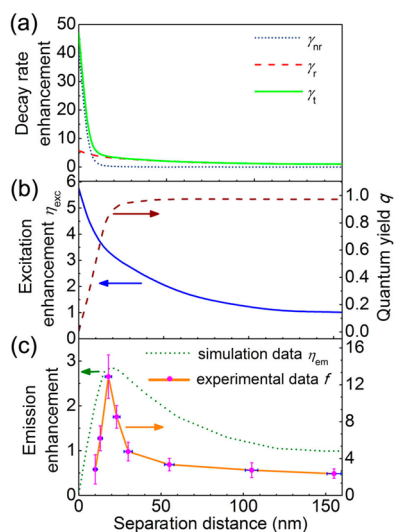


Figure 5. (a) Radiative γ_r , nonradiative γ_{nr} , and total γ_t decay rate enhancement for a point dipole emitter (emission wavelength at 800 nm) above an Au microplate as a function of the separation from the center of the dipole to the surface of Au microplate. (b) Calculated excitation rate enhancement η_{exc} and quantum yield q as a function of the separation distance between the surface of Au microplate and the center of QD. (c) Calculated PL emission enhancement η_{em} as a function of the separation distance. The PL enhancement factor f obtained by experiment is also presented for comparison.

simulation was from the center of the QDs to the surface of the Au microplates taking into account the refraction index of PMMA layers in between. Consequently, the theoretical simulation agreed well with the PL intensity enhancement, reaching the maximum at the separation distance of 18 ± 1.9 nm (namely, 13 ± 1.9 nm PMMA separating layer).

In Figure 5c, it could be also noticed that the maximum PL intensity enhancement for theory was only ~ 3.4 , much lower than that for experiment (~ 16). The theoretical simulation was carried out in the ideal conditions, such as uniform light field distribution in the simulation region, an ideal point dipole emitter to replacing QD, a plane wave light source to replacing the laser with Gaussian beam et al. Furthermore, the absorption efficiency of the QDs to excitation laser and collection efficiency of the objective to the QD fluorescence improved by high reflectance of smooth Au microplate surfaces were also important factors contributing to the difference between the simulated and experimental PL enhancement, which were also the origination that the PL intensity on Au microplates with a 155 nm PMMA film was about 2 times higher than that on glass in Figure 5c, although the near field enhancement effect from Au microplates was almost not active on the QD PL in a so large separation distance. But they were not considered in the theoretical simulation. The different conditions in experiment might cause the large deviation of the maximum PL intensity enhancement from the theoretical simulation.

CONCLUSIONS

Using the single particle spectroscopy, we have investigated the PL behavior of a single CdSeTe/ZnS core-shell QD on a single monocrystal Au microplate with a PMMA separation layer between them. When a QD was directly placed on the surface of Au microplate, the QD PL was completely quenched. By varying the thicknesses of PMMA separating layers, these hybrid structures exhibited enhanced PL intensity as well as

shortened lifetime induced by surface plasmon resonance of Au microplates. A clear effect of distance dependent PL intensity enhancement was observed. The maximum ~ 16 -fold PL enhancement of a single QD was experimentally determined to occur at 18 ± 1.9 nm separation distance between the surface of Au microplate and the center of QD, which showed a good agreement with the theoretical simulation based on FDTD method. Our results indicated that by carefully engineering the separation distance of QDs and Au microplates, the PL dynamics would be changed desirably. This study may pave the way to design nanoscale infrared light sources, sensors, and active devices.

ASSOCIATED CONTENT

Supporting Information

Surface quality examinations of Au microplates, shape and size characterization of the core-shell QDs by TEM and AFM, AFM images and line analysis of an Au microplate without and with an application of about 15 nm PMMA layer, the dispersity of the QDs on a PMMA-covered Au microplate, fluorescence image and spectrum of an Au microplate excited by a 532 nm laser, and a discussion about double exponential decay mechanism of QD fluorescence. This material is available free of charge via the Internet at <http://pubs.acs.org>.

AUTHOR INFORMATION

Corresponding Authors

*(B.W.) E-mail: btwu@phy.ecnu.edu.cn.

*(H.Z.) E-mail: hpzeng@phy.ecnu.edu.cn.

Notes

The authors declare no competing financial interest.

ACKNOWLEDGMENTS

This work was funded in part by the National Nature Science Fund (11104079, 10990101, 61127014, and 91021014), National Special Funds for the Development of Major Scientific Research Instruments and Equipment (61227902), National Key Scientific Instrument Project (2012YQ150072), the Research Fund for the Doctoral Program of Higher Education of China (20110076120019), the Program of Introducing Talents of Discipline to Universities (B12024), the Shanghai Rising-Star Program (13QA1401300), the Shanghai International Cooperation Project (13520720700), and the State Key Laboratory of Luminescent Materials and Devices at South China University of Technology.

REFERENCES

- (1) Atwater, H. A.; Polman, A. Plasmonics for Improved Photovoltaic Devices. *Nat. Mater.* **2010**, *9*, 205–213.
- (2) Anger, P.; Bharadwaj, P.; Novotny, L. Enhancement and Quenching of Single-Molecule Fluorescence. *Phys. Rev. Lett.* **2006**, *96*, 113002.
- (3) Lal, S.; Grady, N. K.; Kundu, J.; Levin, C. S.; Lassiter, J. B.; Halas, N. J. Tailoring Plasmonic Substrates for Surface Enhanced Spectroscopies. *Chem. Soc. Rev.* **2008**, *37*, 898–911.
- (4) Kinkhabwala, A.; Yu, Z.; Fan, S.; Avlasevich, Y.; Muellen, K.; Moerner, W. E. Large Single-Molecule Fluorescence Enhancements Produced by a Bowtie Nanoantenna. *Nat. Photonics* **2009**, *3*, 654–657.
- (5) Wu, E.; Chi, Y. Z.; Wu, B. T.; Xia, K. W.; Yokota, Y.; Ueno, K.; Misawa, H.; Zeng, H. P. Spatial Polarization Sensitivity of Single Au Bowtie Nanostructures. *J. Lumin.* **2011**, *131*, 1971–1974.
- (6) Song, M.; Chen, G. X.; Liu, Y.; Wu, E.; Wu, B. T.; Zeng, H. P. Polarization Properties of Surface Plasmon Enhanced Photoluminescence.

cence from a Single Ag Nanowire. *Opt. Express* **2012**, *20*, 22290–22297.

(7) Li, J. F.; Huang, Y. F.; Ding, Y.; Yang, Z. L.; Li, S. B.; Zhou, X. S.; Fan, F. R.; Zhang, W.; Zhou, Z. Y.; Wu, D. Y.; et al. Shell-Isolated Nanoparticle-Enhanced Raman Spectroscopy. *Nature* **2010**, *464*, 392–395.

(8) Yokota, Y.; Ueno, K.; Misawa, H. Essential Nanogap Effects on Surface-Enhanced Raman Scattering Signals from Closely Spaced Gold Nanoparticles. *Chem. Commun.* **2011**, *47*, 3505–3507.

(9) Kasera, S.; Biedermann, F.; Baumberg, J. J.; Scherman, O. A.; Mahajan, S. Quantitative SERS Using the Sequestration of Small Molecules Inside Precise Plasmonic Nanoconstructs. *Nano Lett.* **2012**, *12*, 5924–5928.

(10) Ueno, K.; Juodkazis, S.; Shibuya, T.; Yokota, Y.; Mizeikis, V.; Sasaki, K.; Misawa, H. Nanoparticle Plasmon-Assisted Two-Photon Polymerization Induced by Incoherent Excitation Source. *J. Am. Chem. Soc.* **2008**, *130*, 6928–6929.

(11) Wu, B. T.; Ueno, K.; Yokota, Y.; Sun, K.; Zeng, H. P.; Misawa, H. Enhancement of a Two-Photon-Induced Reaction in Solution Using Light-Harvesting Gold Nanodimer Structures. *J. Phys. Chem. Lett.* **2012**, *3*, 1443–1447.

(12) Tittel, A.; Yin, X. H.; Giessen, H.; Tian, X. D.; Tian, Z. Q.; Kremers, C.; Chigrin, D. N.; Liu, N. Plasmonic Smart Dust for Probing Local Chemical Reactions. *Nano Lett.* **2013**, *13*, 1816–1821.

(13) Huschka, H.; Zuloaga, J.; Knight, M. W.; Brown, L. V.; Nordlander, P.; Halas, N. J. Light-Induced Release of DNA from Gold Nanoparticles Nanoshells and Nanorods. *J. Am. Chem. Soc.* **2011**, *133*, 12247–12255.

(14) Huang, J.; Jackson, K. S.; Murphy, C. J. Polyelectrolyte Wrapping Layers Control Rates of Photothermal Molecular Release from Gold Nanorods. *Nano Lett.* **2012**, *12*, 2982–2987.

(15) Liu, N.; Tang, M. L.; Hentschel, M.; Giessen, H.; Alivisatos, A. P. Nanoantenna-Enhanced Gas Sensing in a Single Tailored Nanofocus. *Nat. Mater.* **2011**, *10*, 631–636.

(16) Schmidt, M. A.; Lei, D. Y.; Wondraczek, L.; Nazabal, V.; Maier, S. A. Hybrid Nanoparticle-Microcavity-Based Plasmonic Nanosensors with Improved Detection Resolution and Extended Remote-Sensing Ability. *Nat. Commun.* **2012**, *3*, 1–8.

(17) Fang, N.; Lee, H.; Sun, C.; Zhang, X. Sub-Diffraction-Limited Optical Imaging with a Silver Superlens. *Science* **2005**, *308*, 534–537.

(18) Oulton, R. F.; Sorger, V. J.; Zentgraf, T.; Ma, R.; Gladden, C.; Dai, L.; Bartal, G.; Zhang, X. Plasmon Lasers at Deep Subwavelength Scale. *Nature* **2009**, *461*, 629–632.

(19) Akimov, A. V.; Mukherjee, A.; Yu, C. L.; Chang, D. E.; Zibrov, A. S.; Hemmer, P. R.; Park, H.; Lukin, M. D. Generation of single optical plasmons in metallic nanowires coupled to quantum dots. *Nature* **2009**, *450*, 402–406.

(20) Chi, Y. Z.; Chen, G. X.; Jelezko, F.; Wu, E.; Zeng, H. P. Enhanced Photoluminescence of Single-Photon Emitters in Nanodiamonds on a Gold Film. *IEEE Photon. Technol. Lett.* **2011**, *23*, 374–376.

(21) Naiki, H.; Masuo, S.; Machida, S.; Itaya, A. Single-Photon Emission Behavior of Isolated CdSe/ZnS Quantum Dots Interacting with the Localized Surface Plasmon Resonance of Silver Nanoparticles. *J. Phys. Chem. C* **2011**, *115*, 23299–23304.

(22) Shimizu, K. T.; Woo, W. K.; Fisher, B. R.; Eisler, H. J.; Bawendi, M. G. Surface-Enhanced Emission from Single Semiconductor Nanocrystals. *Phys. Rev. Lett.* **2002**, *89*, 117401.

(23) Wu, X. H.; Sun, Y. G.; Pelton, M. Recombination Rates for Single Colloidal Quantum Dots Near a Smooth Metal Film. *Phys. Chem. Chem. Phys.* **2009**, *11*, 5867–5870.

(24) Kulakovich, O.; Strekal, N.; Yaroshevich, A.; Maskevich, S.; Gaponenko, S.; Nabiev, I.; Woggon, U.; Artemyev, M. Enhanced Luminescence of CdSe Quantum Dots on Gold Colloids. *Nano Lett.* **2009**, *2*, 1449–1452.

(25) Vion, C.; Spinicelli, P.; Coolen, L.; Schwob, C.; Frigerio, J. M.; Hermier, J. P.; Maitre, A. Controlled Modification of Single Colloidal CdSe/ZnS Nanocrystal Fluorescence Through Interactions with a Gold Surface. *Opt. Express* **2010**, *18*, 7440–7445.

(26) Mallek-Zouari, I.; Buil, S.; Quelin, X.; Mahler, B.; Dubertret, B.; Hermier, J. P. Plasmon Assisted Single Photon Emission of CdSe/CdS Nanocrystals Deposited on Random Gold Film. *Appl. Phys. Lett.* **2010**, *97*, 053109.

(27) Gomez, D. E.; Vernon, K. C.; Mulvaney, P.; Davis, T. J. Surface Plasmon Mediated Strong Exciton–Photon Coupling in Semiconductor Nanocrystals. *Nano Lett.* **2010**, *10*, 272–274.

(28) Dyadyusha, L.; Yin, H.; Jaiswal, S.; Brown, T.; Baumberg, J. J.; Booy, F. P.; Melvin, T. Quenching of CdSe Quantum Dot emission, a New Approach for Biosensing. *Chem. Commun.* **2005**, *25*, 3201–3203.

(29) Pons, T.; Medintz, I. L.; Sapsford, K. E.; Higashiya, S.; Grimes, A. F.; English, D. S.; Mattoussi, H. On the Quenching of Semiconductor Quantum Dot Photoluminescence by Proximal Gold Nanoparticles. *Nano Lett.* **2007**, *7*, 3157–3164.

(30) Jin, Y. D.; Gao, X. H. Plasmonic Fluorescent Quantum Dots. *Nat. Nanotechnol.* **2009**, *4*, 571–576.

(31) Urena, E. B.; Kreuzer, M. P.; Itzhakov, S.; Rigneault, H.; Quidant, R.; Oron, D.; Wenger, J. Excitation Enhancement of a Quantum Dot Coupled to a Plasmonic Antenna. *Adv. Mater.* **2012**, *24*, 314–320.

(32) Cohen-Hoshen, E.; Bryant, G. W.; Pinkas, I.; Sperling, J.; Bar-Joseph, I. Exciton–Plasmon Interactions in Quantum Dot-Gold Nanoparticle Structures. *Nano Lett.* **2012**, *12*, 4260–4264.

(33) Ratchford, D.; Shafiei, F.; Kim, S.; Gray, S. K.; Li, X. Q. Manipulating Coupling between a Single Semiconductor Quantum Dot and Single Gold Nanoparticle. *Nano Lett.* **2011**, *11*, 1049–1054.

(34) Song, J. H.; Atay, T.; Shi, S. F.; Urabe, H.; Nurmikko, A. V. Large Enhancement of Fluorescence Efficiency From CdSe/ZnS Quantum Dots Induced by Resonant Coupling to Spatially Controlled Surface Plasmons. *Nano Lett.* **2005**, *5*, 1557–1561.

(35) Wei, H.; Ratchford, D.; Li, X. Q.; Xu, H. X.; Shih, C. K. Propagating Surface Plasmon Induced Photon Emission from Quantum Dots. *Nano Lett.* **2009**, *9*, 4168–4171.

(36) Curto, A. G.; Volpe, G.; Taminiu, T. H.; Kreuzer, M. P.; Quidant, R.; van Hulst, N. F. Unidirectional Emission of a Quantum Dot Coupled to a Nanoantenna. *Science* **2010**, *329*, 930–933.

(37) Ma, X. D.; Tan, H.; Kipp, T.; Mews, A. Fluorescence Enhancement, Blinking Suppression, and Gray States of Individual Semiconductor Nanocrystals Close to Gold Nanoparticles. *Nano Lett.* **2010**, *10*, 4166–4174.

(38) Ma, X. D.; Fletcher, K.; Kipp, T.; Grzelczak, M. P.; Wang, Z.; Guerrero-Martinez, A.; Pastoriza-Santos, I.; Kornowski, A.; Liz-Marzan, L. M.; Mews, A. Photoluminescence of Individual Au/CdSe Nanocrystal Complexes with Variable Interparticle Distances. *J. Phys. Chem. Lett.* **2011**, *2*, 2466–2471.

(39) Naiki, H.; Masuhara, A.; Masuo, S.; Onodera, T.; Kasai, H.; Oikawa, H. Highly Controlled Plasmonic Emission Enhancement from Metal-Semiconductor Quantum Dot Complex Nanostructures. *J. Phys. Chem. C* **2013**, *117*, 2455–2459.

(40) Gueroui, Z.; Libchaber, A. Single-Molecule Measurements of Gold-Quenched Quantum Dots. *Phys. Rev. Lett.* **2004**, *93*, 166108.

(41) Matsumoto, Y.; Kanemoto, R.; Itoh, T.; Nakanishi, S.; Ishikawa, M.; Biju, V. Photoluminescence Quenching and Intensity Fluctuations of CdSe-ZnS Quantum Dots on an Ag Nanoparticle Film. *J. Phys. Chem. C* **2008**, *112*, 1345–1350.

(42) Hosoki, K.; Tayagaki, T.; Yamamoto, S.; Matsuda, K.; Kanemitsu, Y. Direct and Stepwise Energy Transfer from Excitons to Plasmons in Close-Packed Metal and Semiconductor Nanoparticle Monolayer Films. *Phys. Rev. Lett.* **2008**, *100*, 207404.

(43) Ueda, A.; Tayagaki, T.; Kanemitsu, Y. Energy Transfer from Semiconductor Nanocrystal Monolayers to Metal Surfaces Revealed by Time-Resolved Photoluminescence Spectroscopy. *Appl. Phys. Lett.* **2008**, *92*, 133118.

(44) Wild, B.; Cao, L. N.; Sun, Y. G.; Khanal, B. P.; Zubarev, E. R.; Gray, S. K.; Scherer, N. F.; Pelton, M. Propagation Lengths and Group Velocities of Plasmons in Chemically Synthesized Gold and Silver Nanowires. *ACS Nano* **2012**, *6*, 472–482.

- (45) Kan, C. X.; Zhu, X. G.; Wang, G. H. Single-Crystalline Gold Microplates Synthesis, Characterization, and Thermal Stability. *J. Phys. Chem. B* **2006**, *110*, 4651–4656.
- (46) Major, T. A.; Devadas, M. S.; Lo, S. S.; Hartland, G. V. Optical and Dynamical Properties of Chemically Synthesized Gold Nanoplates. *J. Phys. Chem. C* **2013**, *117*, 1447–1452.
- (47) Love, J. C.; Demas, J. N. Phase plane method for deconvolution of luminescence decay data with a scattered-light component. *Anal. Chem.* **1984**, *56*, 82–85.
- (48) McKinnon, A. E.; Szabo, A. G.; Miller, D. R. The Deconvolution of Photoluminescence Data. *J. Phys. Chem.* **1977**, *81*, 1564–1570.
- (49) Moskovits, M. Surface-enhanced spectroscopy. *Rev. Mod. Phys.* **1985**, *57*, 783–826.
- (50) Anger, P.; Bharadwaj, P.; Novotny, L. Enhancement and Quenching of Single-Molecule Fluorescence. *Phys. Rev. Lett.* **2006**, *96*, 113002.
- (51) Purcell, E. M. Spontaneous Emission Probabilities at Radio Frequencies. *Phys. Rev.* **1946**, *69*, 681.